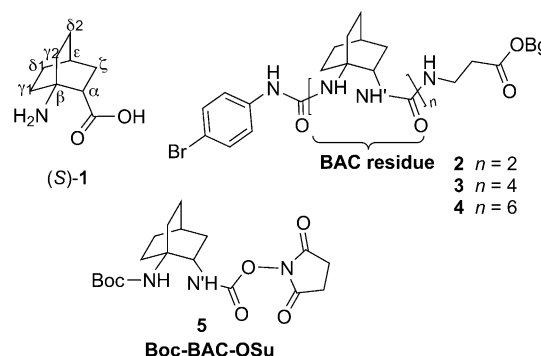


# Robust Helix Formation in a New Family of Oligoureas Based on a Constrained Bicyclic Building Block\*\*

Baptiste Legrand, Christophe André, Emmanuel Wenger, Claude Didierjean, Marie Christine Averlant-Petit, Jean Martinez, Monique Calmes,\* and Muriel Amblard\*

The field of foldamers has become an important area of chemistry over the years because of the particular structural and functional properties that foldamers display. The design, structural properties, and activities of different families of foldamers, including aromatic polyamides or structures closely related to peptides such as peptoids,  $\beta$ -peptides, and  $\gamma$ -peptides, have been exhaustively reviewed.<sup>[1–8]</sup> Among the foldamers based on natural peptide sequences,  $\beta$ -peptides are the most widely studied system. In this system, cyclic  $\beta$ -amino acids are used as building blocks, allowing stabilization of various secondary structures in oligomers by strongly promoting gauche-type torsion angles.<sup>[3,9–12]</sup> Our group has recently described a highly constrained bicyclic  $\beta$ -amino acid, named (*S*)-ABOC **1**, (*S*)-aminobicyclo[2.2.2]octane-2-carboxylic acid (Figure 1).<sup>[13]</sup> This  $\beta^{2,3,3}$ -trisubstituted bicyclic amino acid, able to induce a turn in peptides both in solution and in the solid state,<sup>[14]</sup> displays drastically reduced conformational freedom and a  $\theta_1$  angle locked at approximately 55°. Therefore, this motif is particularly attractive for the design of new foldamers. To stabilize the helical system, other parameters should be considered. Indeed, Guichard and co-workers<sup>[15,16]</sup> provided a useful tool by introducing urea linkages for oligourea foldamers that are  $\gamma$ -peptide mimetics.<sup>[17,18]</sup> The presence of additional nitrogen atoms in the urea linkage promotes helix stabilization by introducing additional conformational restriction to the backbone and hydrogen-bond donor sites.



**Figure 1.** Chemical formulas of (*S*)-ABOC **1**, oligoureas **2**, **3**, **4**, and *N*-Boc-aminobicyclo[2.2.2]octane-2-succinimidyl carbamate **5**.

Although many cyclic  $\beta$ -amino acid oligomers and acyclic urea oligomers have been reported for more than ten years, their combination in a single structure has never been explored. However, such a combination should be a promising approach in the development of a highly stable helix structure, even with few motifs. Thus, we focused on the design of oligomers combining both the benefit of conformationally constrained building blocks and of the bifidic hydrogen-bond stabilization from the urea linkages. In addition, the use of the bicyclo[2.2.2]octane system afforded the first example of a  $C^2, C^{3,3}$ -trisubstitution pattern in the construction of structured oligomers.

To study the progressive folding of bicyclic amino carbamoyl oligomers (BAC oligomers), we synthesized three oligoureas of different lengths ( $n=2, 4, 6$ ). The target oligoureas **2**, **3**, and **4** (Figure 1) were synthesized in solution by stepwise assembly using a standard Boc/Bzl strategy (see Supporting Information for full details). For this purpose, the succinimidyl carbamate derivative **5** (Boc-BAC-OSu), as a precursor of oligourea synthesis, was prepared from Boc-(*S*)-ABOC-OH according to a previously reported procedure.<sup>[19]</sup>

For all oligomers, we used two capping groups, the *N*-benzhydrylglycolamide ester (OBg ester),<sup>[20]</sup> for its ability to induce a folded conformation in short peptides<sup>[21]</sup> and its ability to ease oligomer synthesis, and the 4-bromophenyl group, to favor crystal formation and facilitate phasing. The OBg ester was introduced at the C-terminal end as a  $\beta$ -Ala-OBg residue. This group is orthogonal to Boc and selectively removed under mild alkaline conditions. In addition, it afforded an excellent chromophore that allowed for control of the oligomer synthesis. The 4-bromophenyl group was introduced by way of an isocyanate derivative for capping the N-terminus of oligoureas at the end of the synthesis.

[\*] C. André,<sup>[14]</sup> Prof. J. Martinez, Dr. M. Calmes, Dr. M. Amblard  
Institut des Biomolécules Max Mousseron (IBMM), UMR 5247  
CNRS, Universités Montpellier 1 et 2  
15 avenue Charles Flahault, 34000 Montpellier (France)  
E-mail: monique.calmes@univ-montp2.fr  
muriel.amblard@univ-montp1.fr  
Homepage: <http://www.ibmm.univ-montp1.fr/>  
Dr. B. Legrand,<sup>[14]</sup> Dr. M. C. Averlant-Petit  
Laboratoire de Chimie-Physique Macromoléculaire,  
LCPM—UMR 7568 CNRS Université de Lorraine, 1 rue Grandville,  
54001 Nancy Cedex 1 (France)  
E. Wenger, Dr. C. Didierjean  
Laboratoire de Cristallographie, Résonance Magnétique et Modé-  
lisation, UMR 7063 CNRS Université de Lorraine, Boulevard des  
Aiguillettes, 54506 Vandoeuvre-lès-Nancy Cedex (France)

[†] These authors contributed equally to this work.

[\*\*] We thank the CNRS, MESR and ANR (ANR-08-BLAN-0066-01) for financial support, and the SCBIM and Université de Lorraine for NMR and XRD facilities.

Supporting information for this article (experimental details) is available on the WWW under <http://dx.doi.org/10.1002/anie.201205842>.

The first coupling was performed by adding equimolar amounts of  $\beta$ -Ala-OBg to the activated monomer **5** in the presence of *N,N*-diisopropylethylamine (DIEA). Then, oligoureas **2–4** were prepared by successive Boc deprotection, trifluoroacetate salt (TFA salt) neutralization, and coupling using the activated monomer **5**. After the last coupling and deprotection of the oligomers, one equivalent of 4-bromophenyl isocyanate was added for the final capping step.

NMR spectroscopy studies were conducted on dimer **2**, tetramer **3**, and hexamer **4** in  $\text{CD}_3\text{OH}$ . Despite the repetitive nature of the sequences and the numerous methylene groups on the BAC moiety, the NMR signals were well dispersed (Supporting Information, Figures S2–4). Therefore, nearly all  $^1\text{H}$ ,  $^{13}\text{C}$ , and  $^{15}\text{N}$  resonances could be assigned by combining homonuclear COSY, TOCSY, ROESY experiments and heteronuclear  $^{15}\text{N}$ -HSQC,  $^{13}\text{C}$ -HSQC, and HSQC-TOCSY at  $^{15}\text{N}$  and  $^{13}\text{C}$  natural abundance (Tables S1–6). The high dispersion of the  $^1\text{H}$  NMR signals of the methylene groups of the six BAC residues in peptide **4** is illustrated in the TOCSY spectra (Figures S5–6).

For the three oligoureas, all measurable  $^3J(\text{N'H}, ^\alpha\text{CH})$  coupling constants were  $> 8$  Hz, mostly distributed around 9–10 Hz, which are typical of an anti-periplanar arrangement between the N'H and the  $^\alpha\text{CH}$  protons (Table S7). They indicated a restricted rotation around the  $\text{N}'\text{--}^\alpha\text{C}$  bond.<sup>[15]</sup> Numerous non-sequential NOEs were detected all along the sequence and provided strong evidence for the highly structured nature of the three oligoureas. Characteristic long range NOEs between  $i, i+2$  and  $i, i+3$  residues could be unambiguously assigned. Strong  $^1\text{CH}(i+2)/^\alpha\text{CH}(i)$ , medium or weak  $\text{NH}(i+2)/^\alpha\text{CH}(i)$  and  $\text{N'H}(i+2)/^\alpha\text{CH}(i)$ , and weak  $\text{N'H}(i+3)/^\alpha\text{CH}(i)$  and  $\text{NH}(i+2)/^\alpha\text{CH}(i)$  long range NOE correlations involving BAC methylene protons were detected (Figure 2, Tables S8–10). Interestingly, the  $\text{NH}(i+2)/^\alpha\text{CH}(i)$  and  $\text{N'H}(i+2)/^\alpha\text{CH}(i)$  NOEs had been previously assigned, for oligoureas composed of acyclic motifs, to a minor alternative conformation in methanol but no structure was elucidated.<sup>[22]</sup>

NOEs were used as constraints for the NMR solution structure calculations of **2**, **3**, and **4** using a simulated annealing procedure with AMBER 10 (Figure 3).<sup>[23,24]</sup> For these three oligomers, 26, 49, and 110 unambiguous distance restraints were respectively introduced (inter-residue NOEs are shown in Tables S8–10).

The resulting lowest-energy conformations, considered as the most representative structures for tetramer **3** and hexamer **4**, exhibited a well-defined right-handed 2.5-helix with a pitch around 5.1 Å. Moreover, although dimer **2** was too short to achieve a complete helix turn, numerous NOEs were detected and the calculated structures superimposed well with low RMSD values ( $< 0.3$  Å) when the flexible N-terminal 4-BrPh and C-terminal  $\beta$ -Ala-OBg moieties were omitted (Table S11). The poly-BAC oligomer was stabilized by a regular bifid intramolecular 12- and 14-membered H-bond pseudo-ring network, resulting from  $\text{C=O}(i)\cdots\text{HN}(i+1)$  and  $\text{C=O}(i)\cdots\text{HN}'(i+2)$  hydrogen bonds, forming a right-handed 12/14-helix. The simultaneous presence of 12- and 14-membered pseudocycles was previously shown in *N,N'*-linked oligoureas with proteinogenic side chains.<sup>[15]</sup> Regardless of the

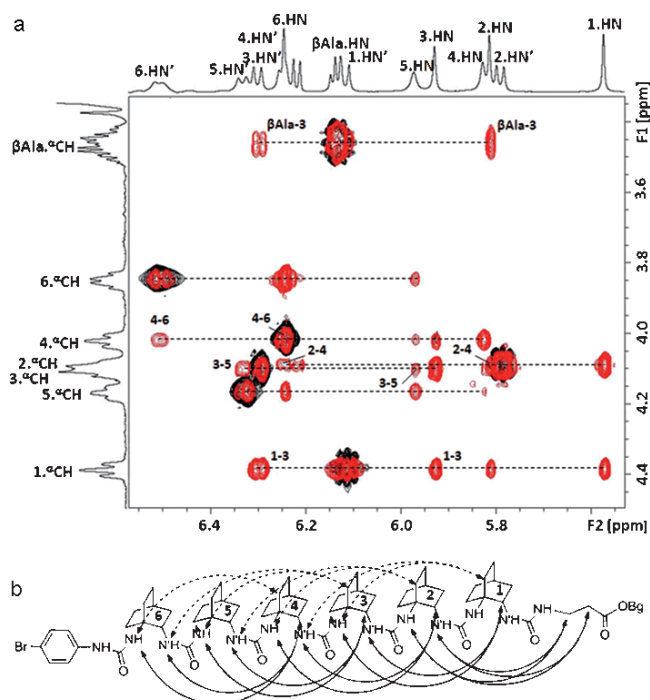


**Figure 2.** a) Superimposition of the  $\text{NH}/^\alpha\text{CH}$  region of the TOCSY (black) and ROESY (red) NMR spectra of the hexamer **4** recorded in  $\text{CD}_3\text{OH}$  at 298 K. Long range  $\text{NH}, \text{N'H}(i+2)/^\alpha\text{CH}(i)$  characteristic NOEs are reported. Other NOE cross-peaks are intra-residual  $\text{HN}'/^\alpha\text{CH}$  and  $\text{HN}/^\alpha\text{CH}$ , and sequential  $\text{HN}(i+1)/^\alpha\text{CH}(i)$ . Numbers shown in the spectra correspond to the BAC residue number shown in (b). b) Unambiguously assigned characteristic long-range NOEs along the hexaurea sequence.

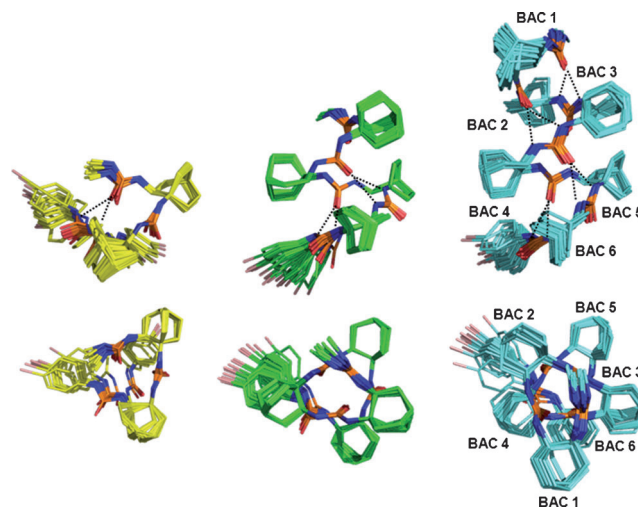


**Figure 3.** Superimposition of the heavy atoms of the backbone of the 20 lowest energy NMR solution structures of dimer **2** (yellow), tetramer **3** (green), and hexamer **4** (cyan). The disordered C-terminal moiety and protons have been omitted for clarity. Dotted lines = hydrogen bonds.

size of the sequences,  $\phi$ ,  $\theta_1$ , and  $\theta_2$  BAC dihedral angles of the three compounds shared remarkably close values, except for the  $\theta_2$  value of the N-terminal BAC residue of each oligourea.

Omitting the N-terminal distortion, the typical average  $\phi$ ,  $\theta_1$ , and  $\theta_2$  values in solution were  $81 \pm 14^\circ$ ,  $51 \pm 6^\circ$ , and  $-102 \pm 13^\circ$ , respectively (Tables S13–15). The solution structures of dimer **2**, tetramer **3**, and hexamer **4** showed great similarity when superimposed (Figure S7). The poly-BAC helix was homogeneous and no critical sequence size was needed to initiate the characteristic 2.5-helical fold, demonstrating the high helical propensity of this sequence type.

In addition, no inconsistent correlations in CD<sub>3</sub>OH were found in the ROESY spectra of the oligoureas **3** and **4**, as has been observed for the oligoureas described by Guichard and co-workers and were assigned to urea-bond *cis-trans* isomerization.<sup>[25]</sup> This result suggested that no isomerization occurred (or could not be detected) showing that the BAC residues induced a high level of rigidity and robustness into the poly-BAC sequences. The bulky bicyclo[2.2.2]octane motif probably prevented the local isomerization of the urea bond by inducing unfavorable steric clashes between the BAC methylene groups and the urea amide protons.

We determined the crystal structures of dimer **2** and tetramer **3'**, corresponding to the methyl ester of **3** (see crystallographic data, Table S12). Partial transesterification of **3** in CH<sub>3</sub>OH during the long crystallization process occurred and led to a crystalline structure of the corresponding methyl ester **3'**. The asymmetric unit of **2** consisted of one molecule while that of **3'** contained two independent molecules exhibiting quite similar structures. The solid-state structures of the dimer and tetramer were globally similar when superimposed on those structures obtained in solution (Figure 4). A similar distortion of the N-terminal end of dimer **2** was observed in both the solution and solid-state structures. Nevertheless, the C-terminal  $\beta$ -Ala-OBg group was disordered in the NMR structures, while a complete turn of the helix could be achieved through a subsequent bifidic hydrogen bond, implicating the carbonyl group of the  $\beta$ -Ala in the crystal structure of **2** (Figure S9).

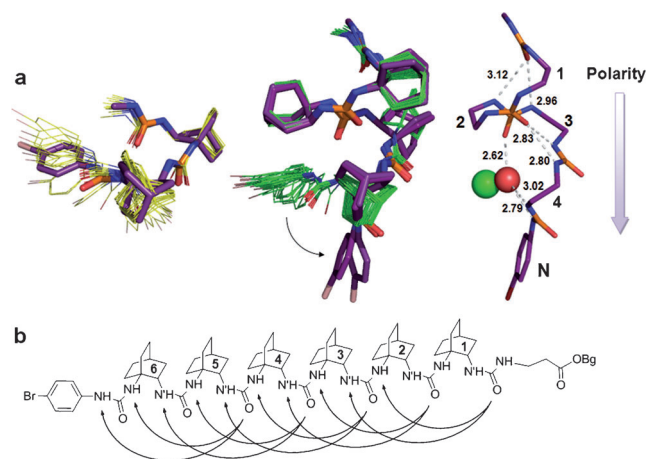


**Figure 4.** a) Superimposition of the NMR (yellow and green) and X-ray crystal (purple) structures of dimer **2** and tetramer **3/3'**. The H-bond network of one X-ray crystal structure of oligomer **3'** is shown at the right. A co-crystallized MeOH molecule is represented by green and red spheres. b) Typical hydrogen-bond pattern defining the oligourea hexamer **4** (12/14 helix).

The crystal structure of **3'** showed a right-handed 2.5-helix with a C- to N-terminal macrodipole. Except for the  $\phi$  angle which exhibited a slight deviation, the dihedral angles of BAC residues in the crystal structures ( $\phi = 63 \pm 6^\circ$ ,  $\theta_1 = 54 \pm 9^\circ$ , and  $\theta_2 = -109 \pm 21^\circ$ ) were close to those measured in solution ( $\phi = 81 \pm 14^\circ$ ,  $\theta_1 = 51 \pm 6^\circ$ , and  $\theta_2 = -102 \pm 13^\circ$ ; Figure S8, Table S15). Notably, the  $\theta_1$  angle value is comparable to that described in the literature for a canonical oligourea helix, while the  $\phi$  and  $\theta_2$  angle values were permuted.<sup>[25,26]</sup>

In addition, a significant difference between the structures of compound **3** in solution and compound **3'** in solid-state could be noticed. The N-terminal moiety of **3'**, because of the insertion of a CH<sub>3</sub>OH molecule, was rotated of approximately  $100^\circ$  ( $\phi$  (BAC **3**) =  $167 \pm 4^\circ$ ) in the solid-state structure. This rotation produced a disruption of the 12- and 14-membered H-bonded ring through the formation of H-bonds between the N-terminal urea and the urea carbonyl group linking BAC moieties 2–3 and the inserted CH<sub>3</sub>OH molecule.

In the crystal structures of both dimer **2** and tetramer **3'**, the molecules stacked into cylindrical columns to maximize the interactions between the boundaries of the helices. This arrangement is generally observed in the solid state of molecules with helices.<sup>[25]</sup> In the crystal of **3'**, all of the columns were oriented in the same direction and their axes coincided with the crystallographic screw axes of the  $P2_1$  space group. Within a column, the stacking of the helical molecules was sinusoidal and a connection between two successive molecules was made through bifurcated hydrogen bonds (Figure S10). In the crystal of **2**, two contiguous columns were upside down in relation to each other (Figure S9). They were held together by bifurcated hydrogen bonds and water molecules. Within a pillar, hydrogen bonds between the carbonyl group of the second urea moiety and the OBg amide group linked the molecules together.

Finally, far-UV (190–260 nm) CD spectra for compounds **2**, **3**, and **4** were recorded in CH<sub>3</sub>OH (Figure 5 and Figure S11). Their CD spectra shared the same shape, with maxima around 205 nm. Interestingly, similar spectra with slightly shifted maxima around 203 nm were obtained for folded oligoureas in an uncapped acyclic series containing at least five residues.<sup>[22]</sup> This CD signature highlighted a similar folding property of both series. However, the CD profile of

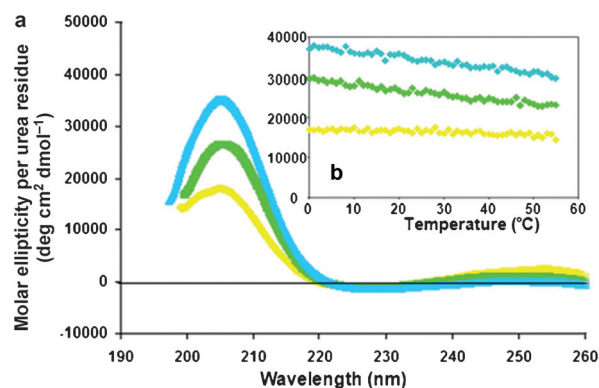


**Figure 5.** a) CD spectra of dimer **2** (yellow), tetramer **3** (green), and hexamer **4** (cyan) recorded at 20°C in CH<sub>3</sub>OH. b) CD signals at  $\lambda_{\text{max}} = 204.8$  nm at variable temperature from 0 to 55°C.



the tetramer with acyclic residues had a broad negative band at approximately 202 nm and did not exhibit the typical profile of folded oligoureases, in contrast to the BAC dimer **2** and tetramer **3**. These results point out again the propensity of the BAC motif to induce a helical structure in oligomers.

For all oligomers, a gradual increase of the temperature, up to 55 °C, induced a slight linear decrease of the maxima of molar ellipticity without variation in the shape of the spectra. When the temperature was returned to 20 °C, a total recovery of the CD signal was observed, suggesting that the limited thermal loss of structure induced by higher temperatures was non-cooperative and fully reversible.

In conclusion, the combination of the constrained bicyclo[2.2.2]octane motif with urea linkages allowed for the development of a highly rigid 2.5<sub>12/14</sub> helical system. All the structural data from the oligoureases indicated the formation of a stable right-handed 2.5-helix with a pitch of 5.1 Å, both in the solution and solid states. The BAC dimer was shown to be a sufficient sequence to initiate helical folding. Compared to oligoureases with acyclic motifs, no *cis-trans* urea-bond isomerization was observed. This conformational feature led to a higher structural rigidity of the BAC homo-oligoureases. For the purpose of developing stable and functional helices, we continue to study the ability of BAC to modulate the stability of hybrid systems consisting of BAC alternating with acyclic residues containing side chains of proteinogenic amino acids. This should provide a particularly attractive molecular architecture for the design of inhibitors of protein–protein interactions because the arrangement of functional groups along the helix surface could be easily controlled.

Received: July 24, 2012

Published online: October 4, 2012

**Keywords:** bicyclo[2.2.2]octane · foldamers · helical structures · NMR spectroscopy · oligoureases

[1] S. H. Gellman, *Acc. Chem. Res.* **1998**, *31*, 173–180.

[2] D. J. Hill, M. J. Mio, R. B. Prince, T. S. Hughes, J. S. Moore, *Chem. Rev.* **2001**, *101*, 3893–4011.

[3] R. P. Cheng, S. H. Gellman, W. F. DeGrado, *Chem. Rev.* **2001**, *101*, 3219–3232.

[4] D. Seebach, A. K. Beck, D. J. Bierbaum, *Chem. Biodiversity* **2004**, *1*, 1111–1239.

[5] C. M. Goodman, S. Choi, S. Shandler, W. F. DeGrado, *Nat. Chem. Biol.* **2007**, *3*, 252–262.

[6] *Foldamers: Structure, Properties, and Applications* (Eds.: S. Hecht, I. Huc), Wiley-VCH, Weinheim, **2007**.

[7] D. Seebach, J. Gardiner, *Acc. Chem. Res.* **2008**, *41*, 1366–1375.

[8] T. A. Martinek, F. Fulop, *Chem. Soc. Rev.* **2012**, *41*, 687–702.

[9] R. J. Doerksen, B. Chen, J. Yuan, J. D. Winkler, M. L. Klein, *Chem. Commun.* **2003**, 2534–2535.

[10] P. G. Vasudev, S. Chatterjee, N. Shamala, P. Balaram, *Acc. Chem. Res.* **2009**, *42*, 1628–1639.

[11] C. Fernandes, S. Faure, E. Pereira, V. Thery, V. Declercq, R. Guillot, D. J. Aitken, *Org. Lett.* **2010**, *12*, 3606–3609.

[12] P. G. Vasudev, S. Chatterjee, N. Shamala, P. Balaram, *Chem. Rev.* **2011**, *111*, 657–687.

[13] O. Songis, C. Didierjean, C. Laurent, J. Martinez, M. Calmes, *Eur. J. Org. Chem.* **2007**, 3166–3172.

[14] C. André, B. Legrand, C. Deng, C. Didierjean, G. Pickaert, J. Martinez, M. C. Averlant-Petit, M. Amblard, M. Calmes, *Org. Lett.* **2012**, *14*, 960–963.

[15] V. Semetey, D. Rognan, C. Hemmerlin, R. Graff, J. P. Briand, M. Marraud, G. Guichard, *Angew. Chem.* **2002**, *114*, 1973–1975; *Angew. Chem. Int. Ed.* **2002**, *41*, 1893–1895.

[16] L. Fischer, G. Guichard, *Org. Biomol. Chem.* **2010**, *8*, 3101–3117.

[17] T. Hintermann, K. Gademann, B. Jaun, D. Seebach, *Helv. Chim. Acta* **1998**, *81*, 983–1002.

[18] L. Guo, W. C. Zhang, A. G. Reidenbach, M. W. Giuliano, I. A. Guzei, L. C. Spencer, S. H. Gellman, *Angew. Chem.* **2011**, *123*, 5965–5968; *Angew. Chem. Int. Ed.* **2011**, *50*, 5843–5846.

[19] V. Semetey, C. Hemmerlin, C. Didierjean, A. P. Schaffner, A. G. Giner, A. Aubry, J. P. Briand, M. Marraud, G. Guichard, *Org. Lett.* **2001**, *3*, 3843–3846.

[20] M. Amblard, M. Rodriguez, J. Martinez, *Tetrahedron* **1988**, *44*, 5101–5108.

[21] M. Crisma, F. Formaggio, P. Ruzza, A. Calderan, S. Elardo, G. Borin, C. Toniolo, *Biopolymers* **2003**, *71*, 17–27.

[22] A. Violette, M. C. Averlant-Petit, V. Semetey, C. Hemmerlin, R. Casimir, R. Graff, M. Marraud, J. P. Briand, D. Rognan, G. Guichard, *J. Am. Chem. Soc.* **2005**, *127*, 2156–2164.

[23] D. A. Case, T. A. Darden, T. E. Cheatham III, C. L. Simmerling, J. Wang, R. E. Duke, R. Luo, M. Crowley, R. C. Walker, W. Zhang, K. M. Merz, B. Wang, S. Hayik, A. Roitberg, G. Seabra, I. Kolossváry, K. F. Wong, F. Paesani, J. Vanicek, X. Wu, S. R. Brozell, T. Steinbrecher, H. Gohlke, L. Yang, C. Tan, J. Mongan, V. Hornak, G. Cui, D. H. Mathews, M. G. Seetin, C. Sagui, V. Babin, P. A. Kollman, AMBER 10, University of California, San Francisco, **2008**.

[24] V. Hornak, R. Abel, A. Okur, B. Strockbine, A. Roitberg, C. Simmerling, *Proteins Struct. Funct. Bioinf.* **2006**, *65*, 712–725.

[25] L. Fischer, P. Claudon, N. Pendem, E. Miclet, C. Didierjean, E. Ennifar, G. Guichard, *Angew. Chem.* **2010**, *122*, 1085–1088; *Angew. Chem. Int. Ed.* **2010**, *49*, 1067–1070.

[26] J. Fremaux, L. Fischer, T. Arbogast, B. Kauffmann, G. Guichard, *Angew. Chem.* **2011**, *123*, 11584–11587; *Angew. Chem. Int. Ed.* **2011**, *50*, 11382–11385.